August 27-31, 2023
FLORENCE - ITALY
ICWE 16
16th International Conference on Wind Engineering

An Investigation to Effect Mechanism of High-order Modes on 3D Coupled Flutter with Modality-driven Method

Jinbo Zhu, Yongxin Yang, Jinjie Zhang, Haojun Xu

State Key Laboratory of Disaster Reduction in Civil Engineering, Tongji University, Shanghai, China, 731366587@qq.com

SUMMARY:
Effect mechanism of high-order modes on multi-mode coupled flutter has been investigated based on the experimental and theoretical analysis. First, an aeroelastic test of a suspension bridge was carried out to learn the participation of each mode in flutter modality. Second, according to the excitation-feedback principle between vibration modes, the practical modality-driven flutter analysis (PMDFA) was proposed to study the quantitative impact of each mode on the three-dimensional (3D) coupled flutter. Then, the system damping was expanded along the span direction by Taylor's formula, and the quantitative relationship between the span section and the aerodynamic performance was established. Finally, the influence of mode participation and its distribution characteristics on the flutter evolution was systematically studied, and the reasons of 3D effect caused by high-order modes were revealed. The research results show that the influence of the second-order positive symmetric heaving mode on the flutter modality is even greater than that of the first-order positive symmetric heaving mode. The damping provided by this second mode changes from negative to positive with wind velocities and its specific impact on flutter depends on the ratio of its own frequency to the system frequency.

Keywords: three-dimensional coupled flutter, high-order mode, modality-driven analysis

1. INTRODUCTION

Bridge flutter is a kind of self-excited divergent vibration with coupled multi modes, which is mainly driven by the basic torsional mode. Due to the coupled effect between modes, each section along the span direction of the bridge shows different motion states, which makes the actual bridge vibration show a strong three-dimensional effect (Ma, 2021). To study the three-dimensional effects, Scanlan (Scanlan, 1978) proposed a three-dimensional flutter frequency domain analysis method based on modal coordinates, but unfortunately this method failed to consider the coupled relationship between modes. Chen (Chen, 2008) extended the closed-form solution of bimodal coupled flutter from 2D to 3D, but this method is only limited to the case of bimodal coupling. At present, the research on the three-dimensional flutter mechanism still remains at the level of the number of participating modes and the similarity of natural modes, and there is no deeper research on how each mode, especially the high-order mode, affects the flutter performance. In this paper, the real participation of high-order modes in flutter modality was determined through experiments. Then, a practical modality-driven flutter analysis method that can reflect the contribution of each mode was proposed to learn the mode effect mechanism. Based on the proposed method, the three-dimensional effects caused by high-order modes and their causes are revealed.

2. EXPERIMENTAL VERIFICATION OF HIGH-ORDER MODAL PARTICIPATION

An aeroelastic experiment of a suspension bridge with the main span of 1860m was carried out in TJ-3 boundary layer wind tunnel of State Key Laboratory of Disaster Reduction in Civil Engineering, Tongji University. Seven measuring points are evenly placed in the direction of the bridge span. The fundamental heaving modes were identified as shown in Fig. 1 (a). The flutter torsional mode is very similar to the first-order positive symmetric torsional mode, while the flutter heaving mode are composed of multiple modes. As shown in Fig. 1 (b), when the participation of the second-order positive symmetric heaving mode (2-S-V) is considered, the similarity between the fitting and actual modes increases from 44.7% to over 90%, which shows the high-order mode (2-S-V) plays an important role in flutter.

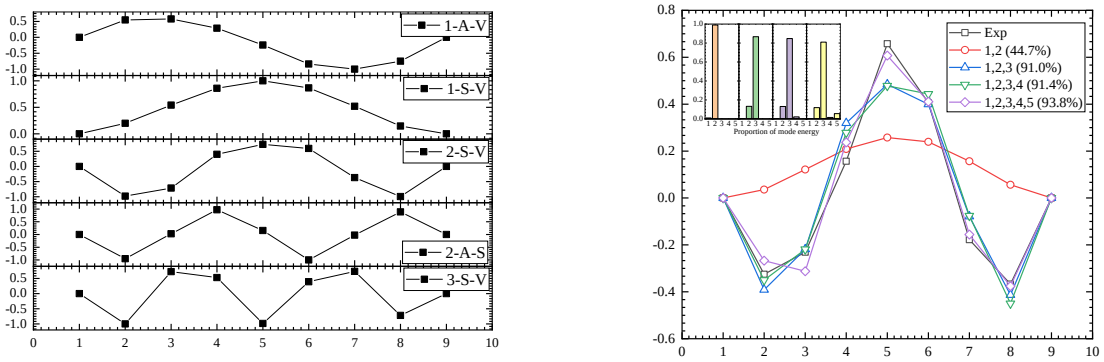

(a) Heaving basic modes (b) Fitted curves by different modes

Figure 1. Basic modes and flutter modality about the heaving motion

3. PRACTICAL MODALITY-DRIVEN FLUTTER ANALYSIS (PMDFA)

Inspired by the excitation-feedback principle between degrees of freedom in 2D flutter analysis (Yang, 2007), this method is introduced into the interaction between main mode and minor modes. Finally, the damping ξ_F and the frequency ω_F of the system are derived as follows:

$$\omega_F = \{\omega_d^2 - \omega_F^2 \cdot Gs_{dd} - \sum_{i=1}^{m} \omega_F^2 \Omega_{id}\{Gs_{di}[Gd_{id}(\sin\theta_{id}^1 + \xi_F \cos\theta_{id}^1) + (Gs_{id} - \xi_F Gd_{id})(\cos\theta_{id}^1 - \xi_F \sin\theta_{id}^1)] + Gd_{di}[Gd_{id}(-\cos\theta_{id}^1 - \xi_F^2 \cos\theta_{id}^1) + (Gs_{id} - \xi_F Gd_{id})(\sin\theta_{id}^1 + \xi_F^2 \sin\theta_{id}^1)]\} \cdot \delta_i / (1 + \xi_F^2)\}^{1/2} \quad (1)$$

$$\xi_F = \frac{\xi_d \omega_d}{\omega_F} - \frac{1}{2} Gd_{dd} - \sum_{i=1}^{m} \frac{\Omega_{id}}{2} [Gd_{di}Gd_{id}(\sin\theta_{id}^1 - 2\xi_F \cos\theta_{id}^1 - \xi_F^2 \sin\theta_{id}^1) + Gd_{di}Gs_{id}(\xi_F \sin\theta_{id}^1 + \cos\theta_{id}^1) + Gs_{di}Gd_{id}(\xi_F \sin\theta_{id}^1 + \cos\theta_{id}^1) - Gs_{di}Gs_{id}\sin\theta_{id}^1] \cdot \delta_i \quad (2)$$

Where $\boldsymbol{Gd}(j,k) = \boldsymbol{\phi}_j^T \boldsymbol{A_D} \boldsymbol{\phi}_k / \boldsymbol{\phi}_j^T \boldsymbol{M_s} \boldsymbol{\phi}_j / \omega_F$, $\boldsymbol{Gs}(j,k) = \boldsymbol{\phi}_j^T \boldsymbol{A_S} \boldsymbol{\phi}_k / \boldsymbol{\phi}_j^T \boldsymbol{M_s} \boldsymbol{\phi}_j / \omega_F^2$, $\boldsymbol{\phi}_j$=j^{th} mode, j, k=1~ m, m =number of modes, $\boldsymbol{M_S}$ = mass matrix, $\boldsymbol{A_D}$ = aerodynamic damping matrix, $\boldsymbol{A_S}$ = aerodynamic stiffness matrix. ω_d = natural frequency of main mode d. ξ_d = natural damping ratio of the main mode. Ω_{id}= dimensionless coefficients. θ_{id}^1, θ_{id}^2= phase angles, i=1~m. δ_i is Dirac-δ function, when $i = d$, $\delta_i = 0$; When $i \neq d$, $\delta_i = 1$.

The damping is the function of $Gd_{ij}^{e_l}$ and $Gs_{ij}^{e_l}$ $(i,j = 1\sim m, l = 1\sim n)$, where e_l indicates the l^{th} segment. The damping variation with wind velocities can be expressed as follows:

$$\Delta\xi_F = \nabla \boldsymbol{G}(\boldsymbol{X}_0)^T \Delta \boldsymbol{X} + \frac{1}{2}\Delta \boldsymbol{X}^T \boldsymbol{H}(\boldsymbol{X}_0)\Delta \boldsymbol{X} + \boldsymbol{o} \tag{3}$$

Where $\boldsymbol{X}_0 = Gs_{11}^{e_1}, \cdots, Gs_{ij}^{e_l}, \cdots, Gd_{11}^{e_1}, \cdots, Gd_{ij}^{e_l}, \cdots$, $\nabla \boldsymbol{G}(\boldsymbol{X}_0)$ is the first-order partial derivative matrix, $\boldsymbol{H}(\boldsymbol{X}_0)$ is the second-order Hessian matrix, and $\boldsymbol{o}$ is the high-order small quantity. Since the iterative wind speed interval is small enough, only the first term in Eq. (3) is considered. The calculation formula of any item related to $Gs_{ij}^{e_l}$ is shown in Eq. (4), and the calculation formula related to $Gd_{ij}^{e_l}$ is similar to Eq. (4).

$$\frac{\partial \xi_F}{\partial Gs_{ij}^{e_l}} = -\frac{{}^{F}Gs_{ij}^{e_l}}{F_{\xi_F}} + \frac{F_{\omega_F}}{F_{\xi_F}} \frac{{}^{D}Gs_{ij}^{e_l}}{D_{\omega_F}} \tag{4}$$

Where D and F indicate Eq. (1) and Eq. (2) respectively. The sum of the relevant terms of e_l indicates the influence of segment l at the current wind velocity. The influence of segment l on the whole flutter process can be obtained by summing the above terms between zero and the flutter critical wind velocity (U_{cr}). Thus, the modality-driven method can not only quantitatively describe the participation of each mode, but also quantify their distribution characteristics.

4. EFFECT MECHANISM OF HIGH-ORDER MODES ON FLUTTER EVOLUTION

Based on PMDFA, the relationship between each mode and flutter performance evolution are investigated from the global and distributed perspectives respectively.

4.1. Global Effect of Each Mode on Flutter Evolution

Compared with the traditional method, the proposed method has been verified to have sufficient accuracy. The 1-S-V, 1-S-T and 2-S-V (expressed by 1, 2, 4 respectively) are the main modes in flutter modality. As shown in Fig. 2 (a) and (b), the damping provided by the high-order mode (2-S-V) falls first and then rises. This mode in the 1500m bridge provides the negative damping in flutter while it provides positive damping in the 500m bridge. As shown in Fig. 2 (c), for the 1500m bridge, the ratios of 1-S-V and 2-S-V frequencies to the system frequency are less than 1 within the flutter critical wind speed. As a result, the denominators of θ_{14}^1 and θ_{24}^1 are less than 0, and these phase angles are in the second quadrant. For 500m bridge, the ratio of 2-S-V frequency to the system frequency is gradually greater than 1 within the flutter critical wind speed, which eventually causes the system damping provided by 2-S-V to change from negative to positive. It is noteworthy that in the case of non-convergence, such as the iteration of 1500m bridge after 91.6m/s, the convergence algorithm needs to be improved (Zhu, 2022).

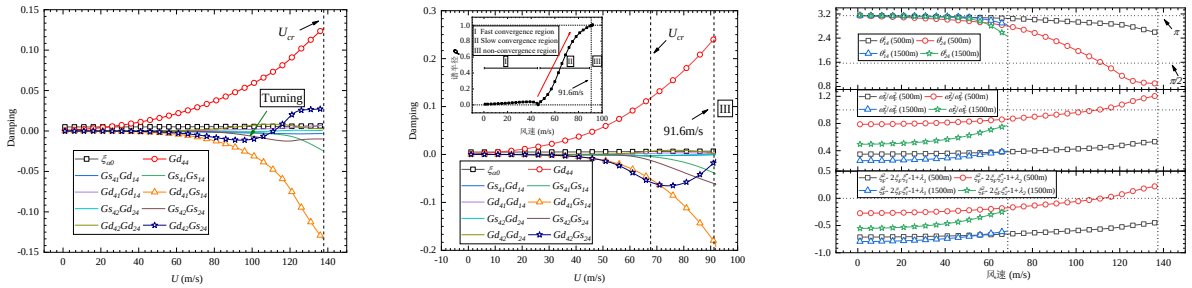

(a) Damping evolution for 500m (b) Damping evolution for 1500m (c) Key parameters

Figure 2. Evolution of damping provided by each mode and key parameters

4.2. Distributed Effect of Each Mode Along Span Direction

Distributed damping of each aerodynamic parameter with wind velocities is shown in Fig. 3 (a) and (b). The upper and lower parts in the figures are the distributions of $Gs_{ij}^{e_l}$ and $Gd_{ij}^{e_l}$. From the contribution of each parameter, Gd_{41}, Gd_{42}, Gd_{44}, Gs_{44}, Gs_{14} and Gs_{24} play a major role in flutter evolution, where Gd_{44} provides maximum positive damping and Gs_{14} or Gs_{24} provides maximum negative damping. The whole distributed damping with wind velocities along the span direction is shown in Fig. 3 (c). Due to the dominant positive damping before $0.8U_{cr}$, the distribution damping shows a half wave and increases with wind velocities. Since the negative damping increases gradually after $0.8U_{cr}$, the damping distribution curve gradually protrudes downward. Since the proportions of negative damping terms are different, the damping distribution of 500m bridge finally shows a half-wave form, while that of 1500m bridge shows a shape of three half waves. Within U_{cr}, about 70% of the beam sections provide almost all aerodynamic damping. That is to say, if aerodynamic countermeasures are adopted to improve flutter performance, only the main contribution areas need to be arranged, not all.

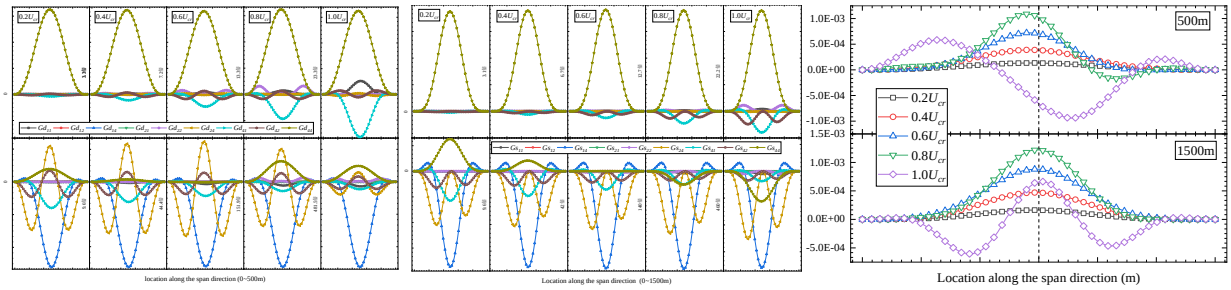

(a) Aerodynamic parameters in 500m (b) Aerodynamic parameters 1500m (c) Distributed damping

Figure 3. Distributed damping along the span direction with wind velocities

5. CONCLUSIONS

The proposed modal analysis method is accurate and reliable. The influence of second-order positive symmetric heaving mode on flutter can even exceed that of first-order positive symmetric heaving mode. About 70% of the beam segments contribute almost all the aerodynamic damping. The effects of high-order modes on flutter are uncertain, which are determined by the ratios of their own frequencies to the system frequency.

ACKNOWLEDGEMENTS

The research is financially supported by National Natural Science Foundation of China (Grant No. 52178503).

REFERENCES

Scanlan, R. H., 1978. The action of flexible bridges under wind: flutter theory. Journal of Sound and Vibration, 60(2): 187-199.

Chen, X, et al, 2008. Identification of critical structural modes and flutter derivatives for predicting coupled bridge flutter. Journal of Wind Engineering and Industrial Aerodynamics, 96(10-11):1856-1870.

Ma, T, et al, 2021. Case study of three-dimensional aeroelastic effect on critical flutter wind speed of long-span bridges. Journal of Wind Engineering and Industrial Aerodynamics, 212(12–15):104614.

Yang, Y., et al, 2007. Investigation on flutter mechanism of long-span bridges with 2d-3DOF method. Wind Struct. 10(5), 421–435.

Zhu, J., et al, 2022. Improvements of convergence robustness with 2D-3DOF method: application of genetic algorithm in coupled flutter. Journal of Bridge Engineering, ASCE 27(10): 04022095.